ACS Partner Journal

Journal of the American Society for Mass Spectrometry

pubs.acs.org/jasms

Research Article

Structures and Chemical Rearrangements of Benzoate Derivatives Following Gas Phase Decarboxylation

Evan H. Perez, Tim Schleif, Joseph P. Messinger, Anna G. Rullán Buxó, Olivia C. Moss, Kim Greis, and Mark A. Johnson*

Cite This: https://doi.org/10.1021/jasms.2c00188

Read Online

ACCESS | Metrics & More | Article Recommendations | Supporting Information

ABSTRACT: Decarboxylation of carboxylate ions in the gas phase provides a useful window into the chemistry displayed by these reactive carbanion intermediates. Here, we explore the species generated by decarboxylation of two benzoate derivatives: 2-formylbenzoate (2FBA) and 2-benzoylbenzoate (2BBA). The nascent product anions are transferred to a cryogenic ion trap where they are cooled to ∼15 K and analyzed by their pattern of vibrational bands obtained with IR photodissociation spectroscopy of weakly bound H_2 molecules. The structures of the quenched species are then determined by comparison of these spectra with those predicted by electronic structure calculations for local minima. The 2-phenide carbanion generated by decarboxylation of 2FBA occurs in two isomeric forms that differ in the orientation of the formyl group, both of which yield a very large (∼110 cm^{-1}) red-shift in the H_2 molecule bound to the anionic carbon center. Although calculated to be a local minimum, the analogous 2-phenide species could not be isolated upon decarboxylation of 2BBA. Rather, the anionic product adopts a ring-closed structure, indicating efficient nucleophilic attack on the pendant phenyl group by the nascent phenide. The barrier for ring closing is evaluated with electronic structure calculations.

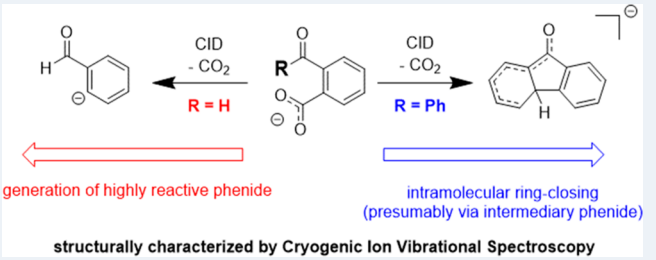

I. INTRODUCTION

The ion chemistry following decarboxylation of deprotonated organic acids is mediated by highly reactive carbanions that undergo a variety of reactions when carried out in the condensed phase.[1,2] The gas-phase analogues, in which carboxylates undergo decarboxylation by collision-induced dissociation (CID), provide a useful way to isolate the carbanions and determine their intrinsic thermochemistry, structure, and reactivity patterns. Early studies include mass spectrometric efforts by Squires and Graul[3,4] and negative-ion photoelectron spectroscopic measurements by the Lineberger group in the 1990s.[6] More recent efforts involve anion vibrational spectroscopy in conjunction with electronic structure calculations to deduce rearrangements. For example, Oomens and co-workers[7,8] used IR multiphoton dissociation of the 300−350 K CID product ions to investigate reactive pathways following decarboxylation. In this paper, we address the nature of the decarboxylation product anion formed upon CID of the 2-formyl- (2FBA, **1**) or 2-benzoylbenzoate (2BBA, **3**) depicted in Scheme 1. Both species are anticipated to generate the phenide motif after heterolytic C−C bond cleavage. The focus of this study is to determine the extent of the intramolecular interactions between the reactive carbanion center and proximal functional groups (H and phenyl, respectively) available in this benzoate scaffold. The nascent product ions are cooled to ∼15 K in a cryogenic ion trap, and the structures of the cold reactant and product anions are deduced by comparing their vibrational spectra with calculated patterns for candidate structures.

Scheme 1. Decarboxylation of Acids via Collision-Induced Dissociation

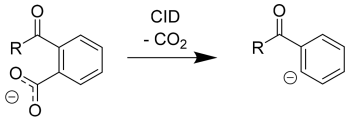

R = H: **1** (2FBA)
R = Ph: **3** (2BBA)

R = H: **2**
R = Ph: **4**

II. EXPERIMENTAL DETAILS AND COMPUTATIONAL METHODS

2-Benzoylbenzoic acid, 2-formylbenzoic acid, acetonitrile (HPLC grade), and water were purchased from Sigma-Aldrich and used without further purification. Helium and hydrogen

Received: July 7, 2022
Revised: August 22, 2022
Accepted: August 22, 2022

were purchased from Air Liquide. The deprotonated anions were generated via electrospray ionization using 1 mM solutions of the respective acids in 1:1 acetonitrile/water. Mass spectra and photofragmentation infrared spectra were collected using a hybrid instrument that combines a commercial ThermoFisher Scientific LTQ Orbitrap Velos with a custom-built, triple-focusing time-of-flight photofragmentation mass spectrometer that has been previously described.[9] In brief, high-resolution mass spectra were collected using the instrument's Orbitrap capability at maximum resolution ($\Delta m/m$ = 100,000), though a reduced resolution of $\Delta m/m$ = 7,500 was used when transferring ions to the photofragmentation spectrometer to maximize ion transmission. Collision-induced dissociation experiments were conducted using the LTQ functionality of the Velos Orbitrap and utilized a normalized collision energy (NCE) of 30 au. All benzoate anions readily undergo decarboxylation in collision-induced dissociation, and loss of 44 u is indeed the dominant fragment in the mass spectra as illustrated in Figures S1 and S2. Weakly bound complexes of the analyte ions and H_2 were formed in a cryogenically cooled ion trap held at ~15 K. Vibrational spectra of the ions were obtained after photodissociation of the H_2-tagged species.

DFT was used to calculate the normal modes of the target ions at the CAM-B3LYP/6-311++G(2d,2p) level of theory. All calculations were conducted using Gaussian 09.[10] Candidate structures were chosen empirically based on the match between the computed frequencies and experimentally observed absorption bands. All energies mentioned throughout the text are evaluated as the sums of the respective electronic energy plus zero-point vibrational energies. Harmonic vibrational frequencies were scaled by 0.953 based on literature scaling factors for the employed level of theory;[11] the H_2 tag vibrations, given their importance for our later analyses, were treated separately by a scaling factor of 0.96 that was determined empirically from matching the calculated H_2 stretching frequency in 2FBA·H_2 to its experimental counterparts.

III. RESULTS AND DISCUSSION

III.A. Vibrational spectra of 2FBA and 2FBA-CO_2: Structural Deformations and H_2 Tag Shifts. To establish the spectral features associated with the parent carboxylate and phenide motifs, we first present the IR photodissociation spectra of 2FBA·H_2 (**1**·H_2) and its decarboxylate, 2FBA-CO_2·H_2 (**2**·H_2), in Figure 1a,c, respectively. In each case, the bands highest in energy (ν^{H_2} at 4078 and 3966 cm^{-1}, respectively) originate from the H_2 stretch of the tag. The former value is typical for H_2 attached to the $-CO_2^-$ headgroup. In the case of carboxylates like acetate and the anion and dianion of dodecanoic acid H_2 is bound to one of the oxygen atoms and points toward it along the H_2 bond axis with a binding energy of ~500 cm^{-1} and frequency of ~4050 cm^{-1}.[12] The much lower frequency of the H_2 stretch in 2FBA-CO_2·H_2 (**2**·H_2), however, indicates that the H_2 molecule is more strongly bound to the carbanion. This qualitative difference is captured in the calculated structures of the two species, which are indicated in the insets in Figure 1a,d. The H_2 molecule in 2FBA-CO_2·H_2 (**2**·H_2) is calculated to be slightly elongated (by 0.007 Å) relative to the value calculated for 2FBA·H_2 (**1**·H_2), accounting for the 112 cm^{-1} red-shift in the H_2 stretch. The H_2 molecule in the 2FBA-CO_2·H_2 (**2**·H_2) complex is calculated to adopt an off-axis docking geometry (by 33 degrees relative to the C^2-C^5 bisector) with an additional tip angle of the H_2 axis (by 18 degrees as indicated in Figure 2d). We note that the H_2 stretching region in the 2FBA-CO_2·H_2 (**2**·H_2) complex appears with smaller bands (labeled *) higher in energy. These are traced to combination bands with soft modes based on the results of two-color, IR-IR isomer-selective spectra (displayed in Figure S3). The physical origin of the large H_2 red shift is discussed further in section III.C.

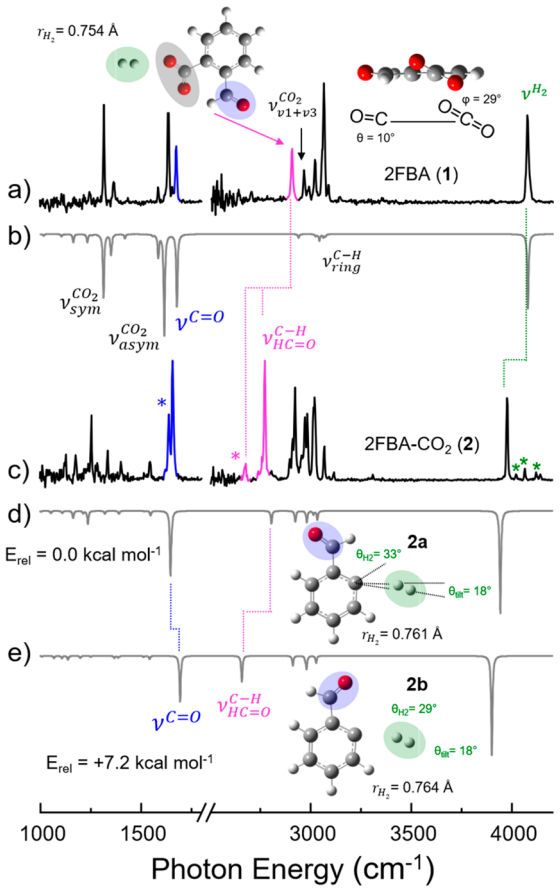

Figure 1. Cryogenically cooled, H_2-tagged vibrational predissociation spectra of (a) 2FBA (**1**), (c) the decarboxylate of 2FBA (**2**) which was generated by collision-induced dissociation of the parent carboxylates. (b) and (d,e) depict the calculated IR spectra of 2FBA (**1**) and the decarboxylate (**2**). The CO stretch fundamentals of the carbonyl groups are highlighted in blue, and the aldehyde CH stretching fundamental is highlighted in pink. Assignments indicated by band labels are detailed in Table 1. Features marked with an asterisk are not reproduced by harmonic frequency calculations (see text). All calculations were performed at the CAM-B3LYP/6-311++G(2d,2p) level of theory.

The much lower frequency of the H_2 stretch in 2FBA-CO_2·H_2 (**2**·H_2), however, indicates that the H_2 molecule is more strongly bound to the carbanion. This qualitative difference is captured in the calculated structures of the two species, which are indicated in the insets in Figure 1a,d. The H_2 molecule in 2FBA-CO_2·H_2 (**2**·H_2) is calculated to be slightly elongated (by 0.007 Å) relative to the value calculated for 2FBA·H_2 (**1**·H_2), accounting for the 112 cm^{-1} red-shift in the H_2 stretch. The H_2 molecule in the 2FBA-CO_2·H_2 (**2**·H_2) complex is calculated to adopt an off-axis docking geometry (by 33 degrees relative to the C^2-C^5 bisector) with an additional tip angle of the H_2 axis (by 18 degrees as indicated in Figure 2d). We note that the H_2 stretching region in the 2FBA-CO_2·H_2 (**2**·H_2) complex appears with smaller bands (labeled *) higher in energy. These are traced to combination bands with soft modes based on the results of two-color, IR-IR isomer-selective spectra (displayed in Figure S3). The physical origin of the large H_2 red shift is discussed further in section III.C.

Returning to 2FBA·H_2 (**2**·H_2), lower in energy, strong bands at 1329 and 1646 cm^{-1} occur in typical positions for the symmetric and asymmetric stretching modes ($\nu_{sym}^{CO_2}$ and $\nu_{asym}^{CO_2}$, respectively) of the CO_2^- group. The band to the blue found at 1676 cm^{-1} is attributed to the C=O ($\nu^{C=O}$) stretching mode. It should be noted that the calculated structure for 2FBA·H_2 (**2**·H_2) provided in Figure 1b was the only low-lying energetic minimum found for this ion. Here, the aldehyde oxygen is pointed away from the carboxylate headgroup. The lowest frequency vibrational mode in the CH stretching region can be attributed to the aldehyde CH stretching fundamental ($\nu_{HC=O}^{C-H}$) at 2904 cm^{-1}. Typical CH stretching fundamentals for benzaldehydes appear at 2700−2900 cm^{-1}.[13]

https://doi.org/10.1021/jasms.2c00188
J. Am. Soc. Mass Spectrom. XXXX, XXX, XXX−XXX

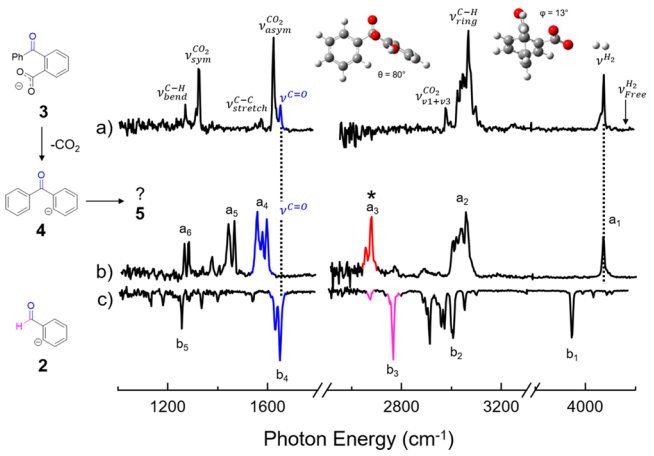

Figure 2. Cryogenically cooled, H_2-tagged vibrational predissociation spectra of (a) 2BBA (**3**), (b) the decarboxylate of 2BBA (**4**), and (c) the decarboxylate of 2FBA (**2**), the latter two of which are generated by collision-induced dissociation of the parent carboxylates. The CO stretch fundamentals of the carbonyl groups are highlighted in blue. The red-shifted CH stretch of the decarboxylate of **3** (marked with an asterisk) is highlighted in red and the aldehyde CH stretches of **2** are highlighted in pink, which are significantly red-shifted from the position in 2FBA·H_2 (**1**·H_2), at 2903 cm^{-1} (Figure 1). The arrow at 4161 cm^{-1} indicates the H_2 stretch frequency of free H_2.[5] Assignments indicated by band labels as well those denoted by letters a_i and b_i are detailed in Table 1.

Figure 1c presents the vibrational spectrum of 2FBA-CO_2·H_2 (**2**·H_2). Following decarboxylation, the carboxylate stretching modes, as expected, are absent. The 2FBA-CO_2·H_2 (**2**·H_2) spectrum displays a close doublet around 1650 cm^{-1}. However, the harmonic calculation for this species only predicts a single feature. This suggests either anharmonic coupling due to higher order terms in the potential or participation of a second isomer. Calculations indicate that the rotamer **2b** arising from the orientation of the formyl group relative to the carbanion center lies 7.2 kcal mol^{-1} above the minimum energy isomer **2a**. These two isomers yield similar bands in the C=O stretching region, but the aldehyde CH modes are calculated to be significantly different, with that in **2b** lying 96 cm^{-1} below the band in **2a**. In fact, two features (at 2672 and 2764 cm^{-1}) are observed in the region where aldehyde CH stretching vibrations would be expected. These are highlighted with a red asterisk in Figure 1c and are consistent with the two-isomer interpretation of the C=O stretch doublet. Although the two rotamers **2a** and **2b** are separated by an activation barrier of 11.8 kcal mol^{-1}, it has been shown that CID can provide enough internal energy[14−16] to fragment ions to accommodate such a rearrangement. Subsequently, the metastable isomer can be trapped behind a significant barrier upon quenching in the cold trap. The higher energy CH stretching region is more populated, appearing as a dense manifold confined to the region 2975−3100 cm^{-1} that occur in the usual range for aromatic CH groups and are observed in both experimental spectra (Figure 1a and 1c). One of these bands falls in the location of the combination band arising from excitation of one quantum in each of the CO stretching modes arising from carboxylate. This band is denoted $\nu^{CO_2}_{\nu1+\nu3}$ in Figure 1a. Although IR forbidden at the harmonic level, this transition is commonly observed in the spectra of decarboxylated anions.[17]

III.B. Vibrational Spectra of 2BBA and 2BBA-CO_2: Structural Rearrangement of the Carbanion. After assigning the spectral signatures of an *ortho*-carboxylate (**1**) and a phenide (**2**) produced by decarboxylation of 2FBA, we next turn to the 2BBA (**3**) system and its decarboxylate. This system was chosen because it provides a richer chemical landscape for intramolecular interactions and opens the possibility of chemical rearrangement. Two views of the calculated structure of **3** are presented as insets in Figure 2a. In contrast to the 2FBA structure, the carboxylate group in **3** resides in the plane of the ring (φ = 4°), similar to the arrangement in the isolated benzoate anion.[18] The angle between the two aromatic rings is calculated to be 80°, consistent with greater steric hindrance afforded by the phenyl group relative to that from the formyl CH. The carbonyl group is predicted to be displaced off ring axis by 13°, suggesting intramolecular repulsion from the proximal carboxylate charge center.

Figure 2a presents the vibrational spectrum of the 2BBA·H_2. Starting highest in energy, the H_2 stretch can be found at nearly the same position as observed for 2FBA·H_2 (8 cm^{-1} difference). The symmetric and asymmetric carboxylate stretches are also very close to those found in 2FBA, as indicated by comparison of the experimental band positions collected in Table 1. The CH stretching region is less congested, revealing the combination band arising from the CO_2^- symmetric and asymmetric stretches, discussed above, as an isolated feature ($\nu^{CO_2}_{\nu1+\nu3}$, Figure 2a). The carbonyl fundamental again lies just above the CO_2^- asymmetric stretch (by 28 cm^{-1}). The significant spectral features of these benzoates are thus preserved in the two benzoate derivatives and are nicely reproduced by the (scaled) calculated frequencies (as are the ones for the respective decarboxylates) with an average deviation of $\Delta\nu$ < 20 cm^{-1} (Table 1).

The 2BBA-CO_2·H_2 vibrational spectrum is displayed in Figure 3b. Most notably, in contrast to the situation found in 2FBA-CO_2·H_2, the H_2 stretching frequency is essentially unperturbed from its position in the 2BBA·H_2 parent spectrum (Table 1). This indicates that the carbanion scaffold is not based on the phenide functionality adopted by 2FBA-CO_2. The characteristic C=O fundamental is also missing in the 2BBA-CO_2·H_2 spectrum, and is replaced by a strong triplet, denoted a_4, centered 150 cm^{-1} lower in energy. Moreover, a new band at 2664 cm^{-1} (a_3) appears far below the aryl C−H stretching modes of 2BBA. The presence of the starkly red-shifted C(sp^3)-H stretching vibration is indicative of a relatively weakly bound hydride such as the one found in HCO_2^- (υ^{CH} = 2449 cm^{-1}).[19] A strongly red-shifted C−H stretch also occurs in the σ-complex resulting from protonation of benzene (υ^{CH} ∼ 2800 cm^{-1}), a binding motif that creates a local sp^3 motif.[20,21] Meanwhile, redshifts in carbonyl C=O stretch are indicative of electron density being displaced into the antibonding π^* orbital, resulting in bond elongation. Taken altogether, these spectral changes indicate that a significant structural rearrangement has occurred in the carbanion generated by decarboxylation. Such skeletal rearrangements of closed-shell anions in gas-phase have been extensively investigated by Bowie et al. as summarized in their review,[22] with the one reported here being reminiscent of the formation of fluorenylanions from Ph_2CH^- proposed by them.[23]

An ion containing the phenide motif **4** was optimized as a local minimum, with the structure and harmonic spectrum presented in Figure S4. This geometry is predicted to yield

https://doi.org/10.1021/jasms.2c00188
J. Am. Soc. Mass Spectrom. XXXX, XXX, XXX−XXX

Table 1. Experimental (± 4 cm^{-1}) Bands (Bold), Harmonic Frequencies (in Parentheses, Scaled by 0.953), and Mode Character Assignments/Labels for the Computed Spectra[a]

Label/Assignment	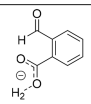 2FBA·H_2 (**1**)	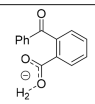 2BBA·H_2 (**3**)	 2FBA-CO_2·H_2 (**2a**)	 2BBA-CO_2·H_2 (**5**)
ν^{H_2} [a_1 / b_1]	**4069** (4044.2)	**4077** (4054.7)	**3964** (3905.8)	**4066** (4064.3)
ν_{ring}^{C-H} [a_2 / b_2]	**2959, 2986, 3015, 3059, 3084** (3020.7, 3039.2, 3059.1, 3069.2)	**2971-3094** (3008.0-3088.5)	**2917, 2968, 3010, 3062** (2919.5, 2978.0, 3010.2, 3029.5)	**2996-3049** (2993.1-3049.7)
$\nu_{HC=O}^{C-H}$ [b_3]	**2903** (2936.7)	**N/A** (N/A)	**2672, 2764** (2803.1)	**N/A** (N/A)
$\nu^{C=O}$ [a_4 / b_4]	**1675** (1678.7)	**1663** (1665.3)	**1637, 1659** (1650.0)	**1560** (1553.0)
$\nu_{sp^3}^{C-H}$ [a_3]	**N/A** (N/A)	**N/A** (N/A)	**N/A** (N/A)	**2667** (2709.4)
$\nu_{ring}^{sym\ C=C}$	**1584** (1588.2)	**1559, 1584** (1565.2, 1588.5)	**1546** (1549.4)	**1581, 1597** (1586.3, 1598.3)
$\nu_{ring\ bend}^{C-H}$ [a_5 / b_5]	**1317** (1316.3)	**1271** (1219.6, 1247.3, 1270.2)	**1129, 1173, 1251, 1397, 1543** (1112.5, 1164.5, 1235.3, 1393.9, 1549.4)	**1439, 1464** (1440.0, 1452.7)
$\nu^{asym\ CO_2}$	**1635** (1617.7)	**1635** (1620.3)	**N/A** (N/A)	**N/A** (N/A)
$\nu^{sym\ CO_2}$	**1317** (1316.3)	**1326** (1330.8)	**N/A** (N/A)	**N/A** (N/A)
$\nu_{bends}^{C-H,\ aldehyde}$	**1364** (1353.8)	**N/A** (N/A)	**1336** (1323.0)	**N/A** (N/A)
$\nu_{sp^3\ bend}^{C-H}$ [a_6]	**N/A** (N/A)	**N/A** (N/A)	**N/A** (N/A)	**1259, 1277** (1248.8)

[a]All calculations were performed at the CAM-B3LYP/6-311G++(2d,2p) level of theory.

similar spectral features as those found in 2FBA-CO_2, e.g., with a typical carbonyl fundamental frequency and a strongly red-shifted H_2 stretch. This pattern is not consistent with the observed 2BBA-CO_2 spectrum (Figure 2c). However, an isomer **5** significantly lower in energy was found with the structure indicated in the inset of Figure 3a. This isomer is connected to phenide **4** by an activation barrier of 11.2 kcal mol^{-1} and stems from the nucleophilic attack of the negative charge center on the pendant phenyl ring. Similar rearrangements of the benzophenone scaffold have previously been observed in the gas phase for positively charged ions and in the condensed phase.[24,25] The calculated spectrum for **5** (Figure 3c) indeed reproduces the experimentally observed band pattern of the 2BBA-CO_2 product ion. Specifically, peak a_3, the red-shifted feature at 2664 cm^{-1}, is traced to the C−H stretch of the sp^3-hybridized carbon resulting from the ring-closing reaction. The triplet motif of the red-shifted C═O band is accounted for by mixing with proximal C═C stretching modes. Note that **5** is the only species formed upon decarboxylation of 2BBA, indicating that the ring-closing reaction is rapid under our experimental conditions.

III.C. Anion Dependence of the H_2 Frequency Shifts.

Having elucidated the structures of the **2a**, **4**, and **5** anions, it is useful to consider the cause of the differing redshifts displayed by the H_2 adducts in each. A comparison of the electronic density maps of these species is displayed in Figure 4. It is evident that the negative charge in **5** resides primarily on the carbonyl group, which is indeed the docking site for the H_2 molecule (see structure in Figure 3b). This concentration of excess charge is consistent with the redshift in the C═O stretch from 2BBA (**3**) to **5**, which reflects the increase in length of the C═O bond from 1.21 to 1.24 Å. In both phenide

https://doi.org/10.1021/jasms.2c00188
J. Am. Soc. Mass Spectrom. XXXX, XXX, XXX−XXX

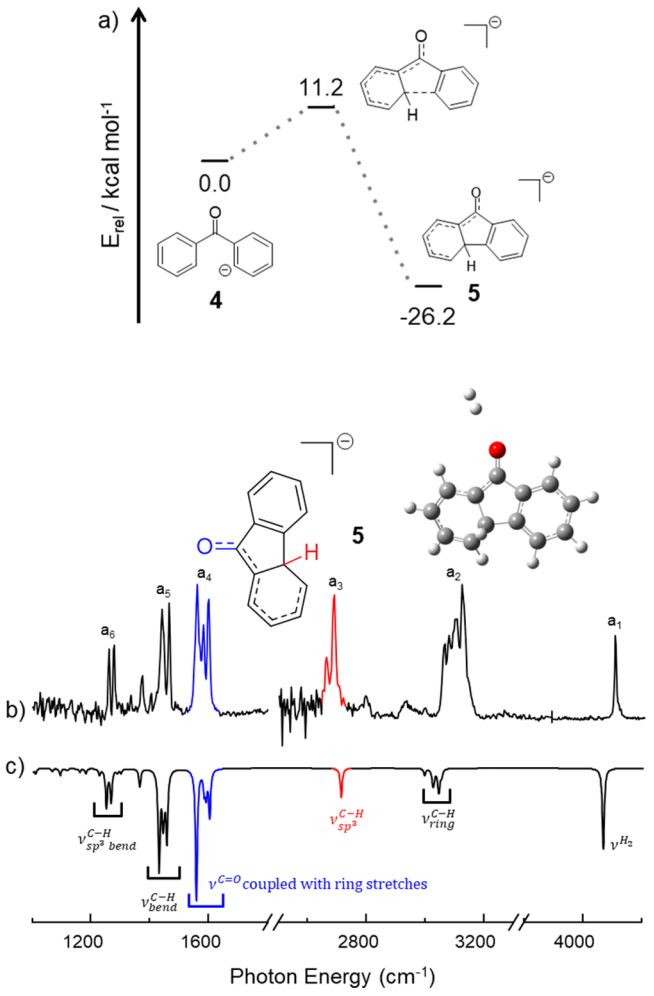

Figure 3. (a) Potential energy diagram for the chemical tranformation of the phenide ion (**4**) to the fluorenone-like ring closed product (**5**). (b) Experimental IR spectrum of the H_2-tagged 2BBA decarboxylate at 15 K, compared to the (scaled) computed vibrational spectrum predicted for the ring closed structure **5** (c). The CO stretch, coupled to various ring stretches, is highlighted in blue and the sp^3 CH stretch is highlighted in red. Band assignments are located in Table 1. All calculations were performed at the CAM-B3LYP/6-311++G(2d,2p) level of theory.

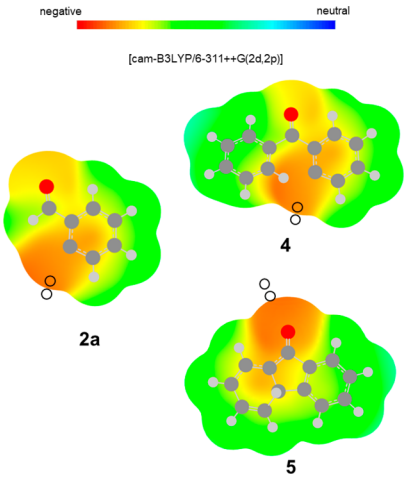

Figure 4. Plots of the electrostatic potential on the respective 0.02 a_0^{-3} isosurfaces of the more stable rotamer of 2FBA-CO_2 (**2a**), the fluorenone-like ring-closed product (**5**), and its phenide isomer (**4**, not observed experimentally). The color code corresponds to red, negative potential = −0.2; blue, potential = 0. Black circles indicate the calculated position of the H_2 complexes. All calculations were performed at the CAM-B3LYP/6-311++G(2d,2p) level of theory.

264 and ring-closed anions, H_2 attaches to the position of highest
265 negative charge density. However, the degree of charge
266 localization is calculated to be comparable in **2**, **4**, and **5**
267 (Figure 4), while the H_2 stretch is observed to be strongly red-
268 shifted (by ∼100 cm^{-1}) in the phenide species **2** compared to
269 **5** (s. Table 1). Consequently, the origin of the shift is not
270 primarily due to electrostatics. Rather, it likely reflects a
271 chemical interaction with the carbanion center in the phenide
272 motif, similar to that which drives nucleophilic attack and C−C
273 bond formation leading to **5**. In the case of H_2, this would lead
274 to C−H bond formation with loss of H^-. The exit channel of
275 the latter would correspond to the H^--benzaldehyde ion−
276 molecule complex. This raises an interesting speculation that
277 reaction of H^- with benzaldehyde could generate **2** by
278 elimination of H_2. To further explore this point, we calculated
279 the potential surface corresponding to H_2 attacking the
280 carbanion center in **2**. This was accomplished by scanning
281 the C−H distance while relaxing all other coordinates. The
f5 282 resulting profiles for H_2 approach to both 2FBA-CO_2 isomers
(**2a** and **2b**) are displayed in Figure 5. These curves reveal a 283 f5
scenario in which, after crossing a barrier of ∼9 kcal mol^{-1}, the 284

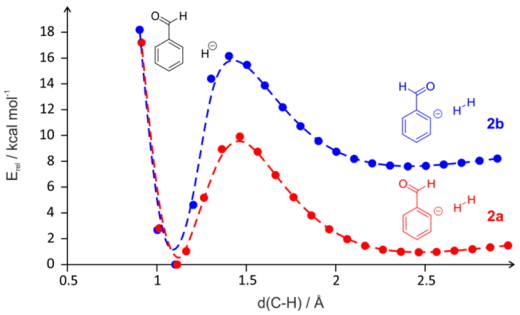

Figure 5. Potential energy curve describing the reactive encounter of H_2 with 2FBA-CO_2 (**2**). After a shallow minimum corresponding to the relatively weakly bound "tagging" regime with a minimum near 2.5 Å, a second minimum is recovered upon C−H bond formation to yield the $\bar{H}$ adduct with benzaldehyde. All calculations were performed at the CAM-B3LYP/6-311++G(2d,2p) level of theory.

systems adopt a minimum energy structure corresponding to 285
the $\bar{H}$-benzaldehyde ion−molecule complex. In this context, 286
the anomalous redshift in the H_2 frequencies displayed by the 287
phenide-H_2 adducts reflects this low-lying reaction pathway, 288
where the H_2 "tag" actually resides in this ion−molecule 289
reaction's entrance channel complex. Along these lines, the 290
tricyclic structure of **5** is interestingly reminiscent of the 291
fluorenone scaffold, which would be generated by loss of 292
hydride from the sp^3 carbon atom. These considerations 293
suggest that a fruitful future direction for further research 294
would be the characterization of the bimolecular reaction 295
chemistry of carbanions generated by decarboxylation of the 296
ring isomers of benzoate derivatives. Of particular interest, for 297
example, is the nature of the 3- and 4-BBA-CO_2 species, which 298
introduce the possibility of trapping the phenide motif 299
depending on the barrier for circumambulatory migration of 300
the carbanion charge center around the ring. 301

https://doi.org/10.1021/jasms.2c00188
J. Am. Soc. Mass Spectrom. XXXX, XXX, XXX−XXX

IV. SUMMARY

Collisional decarboxylation of 2-benzoylbenzoate and 2-formylbenzoate anions provides a platform to characterize chemical and structural rearrangements that occur in the fragment carbanions. The structures of the decarboxylates were determined by cooling them to ∼15 K in a buffer gas cooled cryogenic ion trap and recording their vibrational spectra with IR photodissociation of H_2 "tag" molecules. Decarboxylation of 2-benzoylbenzoate is observed to exclusively undergo a ring-closing reaction involving C−C bond formation to the proximal phenyl group. The fact that the metastable phenide cannot be isolated after CID indicates that this nascent species is created with internal energy significantly greater than the calculated barrier of 11.2 kcal mol^{-1}. The resulting tricyclic structure has several distinct spectroscopic features relative to those arising from the charge-localized (phenide) motif adopted by the decarboxylate of 2-formylbenzoate. These include a much smaller redshift of the weakly bound H_2 stretch and a very strongly red-shifted CH stretch fundamental that is traced to the CH group located on the sp^3 carbon center at the apex of two rings. The different spectroscopic response of the H_2 adducts is consistent with a scenario where the ring-closed product is less reactive toward the H_2 tag than the exposed charge center on a single carbon atom in the phenide motif.

■ ASSOCIATED CONTENT

Supporting Information

The Supporting Information is available free of charge at https://pubs.acs.org/doi/10.1021/jasms.2c00188.

High-resolution mass spectrometry of 2-benzoylbenzoate, 2-formylbenzoate, and their respective decarboxylates (Figures S1 and S2), two-color IR laser experiment of the decarboxylate of H_2-tagged 2-formylbenzoate (Figure S3), detailed analysis of experimental IR spectrum of the decarboxylate of H_2-tagged 2-benzoylbenzoate (Figure S4), and Cartesian coordinates of calculated structures (Tables S1−S11) (PDF)

■ AUTHOR INFORMATION

Corresponding Author

Mark A. Johnson − *Sterling Chemistry Laboratory, Department of Chemistry, Yale University, New Haven, Connecticut 06520, United States;* orcid.org/0000-0002-1492-6993; Email: mark.johnson@yale.edu

Authors

Evan H. Perez − *Sterling Chemistry Laboratory, Department of Chemistry, Yale University, New Haven, Connecticut 06520, United States;* orcid.org/0000-0002-0837-4723

Tim Schleif − *Sterling Chemistry Laboratory, Department of Chemistry, Yale University, New Haven, Connecticut 06520, United States;* orcid.org/0000-0003-0154-9540

Joseph P. Messinger − *Sterling Chemistry Laboratory, Department of Chemistry, Yale University, New Haven, Connecticut 06520, United States;* orcid.org/0000-0001-7305-3945

Anna G. Rullán Buxó − *Sterling Chemistry Laboratory, Department of Chemistry, Yale University, New Haven, Connecticut 06520, United States*

Olivia C. Moss − *Sterling Chemistry Laboratory, Department of Chemistry, Yale University, New Haven, Connecticut 06520, United States;* orcid.org/0000-0001-9434-2965

Kim Greis − *Sterling Chemistry Laboratory, Department of Chemistry, Yale University, New Haven, Connecticut 06520, United States; Institut für Chemie und Biochemie, Freie Universität Berlin, 14195 Berlin, Germany; Fritz-Haber-Institut der Max-Planck-Gesellschaft, 14195 Berlin, Germany;* orcid.org/0000-0002-9107-2282

Complete contact information is available at: https://pubs.acs.org/10.1021/jasms.2c00188

Notes

The authors declare no competing financial interest.

■ ACKNOWLEDGMENTS

We thank the Air Force Office of Scientific research under AFOSR Award No. FA9550-18-1-0213 for support of our work on the dynamics of CO_2 activation reactions. J.M., E.H.P., A.G.R.B., and O.M. were supported by the NSF Center for Aerosol Impacts on Chemistry of the Environment (CAICE) for support of the aspect of this work (CHE-1801971) related to the photophysics of 4BBA as a proxy molecule for sea spray aerosol radical initiation species. A.G.R.B. was also supported partially by the Yale STARS program, which provides research opportunities for URM students in STEM fields. T.S. was supported by a Walter-Benjamin Scholarship by the Deutsche Forschungsgemeinschaft (Projektnummer 459401225). K.G. thanks the Fonds National de la Recherche, Luxembourg, for funding the project GlycoCat (13549747) and the Fulbright Program for funding his research stay at Yale University.

■ REFERENCES

(1) O'Hair, R.; Rijs, N. Gas Phase Studies of the Pesci Decarboxylation Reaction: Synthesis, Structure, and Unimolecular and Bimolecular Reactivity of Organometallic Ions. *Acc. Chem. Res.* **2015**, *48* (2), 329−340.

(2) Tian, Z.; Kass, S. Carbanions in the Gas Phase. *Chem. Rev.* **2013**, *113* (9), 6986−7010.

(3) Graul, S. T.; Squires, R. R. On the Existence of Alkyl Carbanions in the Gas-Phase. *J. Am. Chem. Soc.* **1988**, *110* (2), 607−608.

(4) Squires, R. R. Gas-Phase Carbanion Chemistry. *Acc. Chem. Res.* **1992**, *25* (10), 461−467.

(5) Dickenson, G. D.; Niu, M. L.; Salumbides, E. J.; Komasa, J.; Eikema, K. S. E.; Pachucki, K.; Ubachs, W. Fundamental Vibration of Molecular Hydrogen. *Phys. Rev. Lett.* **2013**, *110* (19), 193601.

(6) Lineberger, W.; Johnson, M.; Martinez, T. Once upon Anion: A Tale of Photodetachment. *Annu. Rev. Phys. Chem.* **2013**, *64*, 21−36.

(7) Paul, M.; Peckelsen, K.; Thomulka, T.; Neudorfl, J.; Martens, J.; Berden, G.; Oomens, J.; Berkessel, A.; Meijer, A.; Schafer, M. Hydrogen tunneling avoided: enol-formation from a charge-tagged phenyl pyruvic acid derivative evidenced by tandem-MS, IR ion spectroscopy and theory. *Phys. Chem. Chem. Phys.* **2019**, *21* (30), 16591−16600.

(8) Schafer, M.; Peckelsen, K.; Paul, M.; Martens, J.; Oomens, J.; Berden, G.; Berkessel, A.; Meijer, A. Hydrogen Tunneling above Room Temperature Evidenced by Infrared Ion Spectroscopy. *J. Am. Chem. Soc.* **2017**, *139* (16), 5779−5786.

(9) Menges, F. S.; Perez, E. H.; Edington, S. C.; Duong, C. H.; Yang, N.; Johnson, M. A. Integration of High-Resolution Mass Spectrometry with Cryogenic Ion Vibrational Spectroscopy. *J. Am. Soc. Mass Spectrom.* **2019**, *30* (9), 1551−1557.

(10) Frisch, M. J.; Trucks, G. W.; Schlegel, H. B.; Scuseria, G. E.; Robb, M. A.; Cheeseman, J. R.; Scalmani, G.; Barone, V.; Mennucci, B.; Petersson, G. A.; Nakatsuji, H.; Caricato, M.; Li, X.; Hratchian, H. P.; Izmaylov, A. F.; Bloino, J.; Zheng, G.; Sonnenberg, J. L.; Hada, M.; Ehara, M.; Toyota, K.; Fukuda, R.; Hasegawa, J.; Ishida, M.; Nakajima, T.; Honda, Y.; Kitao, O.; Nakai, H.; Vreven, T.;

Montgomery, J. A., Jr.; Peralta, J. E.; Ogliaro, F.; Bearpark, M.; Heyd, J. J.; Brothers, E.; Kudin, K. N.; Staroverov, V. N.; Kobayashi, R.; Normand, J.; Raghavachari, K.; Rendell, A.; Burant, J. C.; Iyengar, S. S.; Tomasi, J.; Cossi, M.; Rega, N.; Millam, J. M.; Klene, M.; Knox, J. E.; Cross, J. B.; Bakken, V.; Adamo, C.; Jaramillo, J.; Gomperts, R.; Stratmann, R. E.; Yazyev, O.; Austin, A. J.; Cammi, R.; Pomelli, C.; Ochterski, J. W.; Martin, R. L.; Morokuma, K.; Zakrzewski, V. G.; Voth, G. A.; Salvador, P.; Dannenberg, J. J.; Dapprich, S.; Daniels, A. D.; Farkas, Ö.; Foresman, J. B.; Ortiz, J. V.; Cioslowski, J.; Fox, D. J. *Gaussian 09, Revision D.01*; Gaussian, Inc.: Wallingford, CT, 2009.

(11) Kashinski, D. O.; Chase, G. M.; Nelson, R. G.; Di Nallo, O. E.; Scales, A. N.; VanderLey, D. L.; Byrd, E. F. C. Harmonic Vibrational Frequencies: Approximate Global Scaling Factors for TPSS, M06, and M11 Functional Families Using Several Common Basis Sets. *J. Phys. Chem. A* **2017**, *121* (11), 2265−2273.

(12) Kamrath, M. Z.; Relph, R. A.; Guasco, T. L.; Leavitt, C. M.; Johnson, M. A. Vibrational Predissociation Spectroscopy of the H_2-Tagged Mono- and Dicarboxylate Anions of Dodecanedioic Acid. *Int. J. Mass Spectrom.* **2011**, *300* (2−3), 91−98.

(13) Tolstorozhev, G. B.; Skornyakov, I. V.; Bel'kov, M. V.; Shadyro, O. I.; Brinkevich, S. D.; Samovich, S. N. IR spectra of benzaldehyde and its derivatives in different aggregate states. *Opt. Spectrosc.* **2012**, *113* (2), 179−183.

(14) Louris, J. N.; Cooks, R. G.; Syka, J. E. P.; Kelley, P. E.; Stafford, G. C.; Todd, J. F. J. Instrumentation, Applications, and Energy Deposition in Quadrupole Ion-Trap Tandem Mass-Spectrometry. *Anal. Chem.* **1987**, *59* (13), 1677−1685.

(15) Molesworth, S.; Leavitt, C. M.; Groenewold, G. S.; Oomens, J.; Steill, J. D.; van Stipdonk, M. Spectroscopic Evidence for Mobilization of Amide Position Protons During CID of Model Peptide Ions. *J. Am. Soc. Mass Spectrom.* **2009**, *20* (10), 1841−1845.

(16) Harrilal, C. P.; DeBlase, A. F.; Fischer, J. L.; Lawler, J. T.; McLuckey, S. A.; Zwier, T. S. Infrared Population Transfer Spectroscopy of Cryo-Cooled Ions: Quantitative Tests of the Effects of Collisional Cooling on the Room Temperature Conformer Populations. *J. Phys. Chem. A* **2018**, *122* (8), 2096−2107.

(17) Shin, J.-W.; Hammer, N. I.; Johnson, M. A.; Schneider, H.; Gloss, A.; Weber, J. M. An Infrared Investigation of the $(CO_2)_n^-$ Clusters: Core Ion Switching from Both the Ion and Solvent Perspectives. *J. Phys. Chem. A* **2005**, *109*, 3146−3152.

(18) Woo, H. K.; Wang, X. B.; Kiran, B.; Wang, L. S. Temperature-dependent photoelectron spectroscopy of methyl benzoate anions: Observation of steric effect in o-methyl benzoate. *J. Phys. Chem. A* **2005**, *109* (50), 11395−11400.

(19) Gerardi, H. K.; DeBlase, A. F.; Su, X.; Jordan, K. D.; McCoy, A. B.; Johnson, M. A. Unraveling the Anomalous Solvatochromic Response of the Formate Ion Vibrational Spectrum: An Infrared, Ar-Tagging Study of the HCO_2^-, DCO_2^-, and $HCO_2^-{\cdot}H_2O$ Ions. *J. Phys. Chem. Lett.* **2011**, *2* (19), 2437−2441.

(20) Solcà, N.; Dopfer, O. Protonated Benzene: IR Spectrum and Structure of C6H7+. *Angew. Chem., Int. Ed.* **2002**, *41* (19), 3628−3631.

(21) Douberly, G. E.; Ricks, A. M.; Schleyer, P. v. R.; Duncan, M. A. Infrared Spectroscopy of Gas Phase Benzenium Ions: Protonated Benzene and Protonated Toluene, from 750 to 3400 cm−1. *J. Phys. Chem. A* **2008**, *112* (22), 4869−4874.

(22) Eichinger, P. C. H.; Dua, S.; Bowie, J. H. A Comparison of Skeletal Rearrangement Reactions of Even-Electron Anions in Solution and in the Gas-Phase. *Int. J. Mass Spectrom.* **1994**, *133* (1), 1−12.

(23) Currie, G. J.; Bowie, J. H.; Massywestropp, R. A.; Adams, G. W. Collision-Induced Dissociations of Substituted Benzyl Negative-Ions in the Gas-Phase - the Elimination of C4h4. *J. Chem. Soc., Perkin Trans. 2* **1988**, No. 3, 403−408.

(24) Amundson, L. M.; Owen, B. C.; Gallardo, V. A.; Habicht, S. C.; Fu, M. K.; Shea, R. C.; Mossman, A. B.; Kenttamaa, H. I. Differentiation of Regioisomeric Aromatic Ketocarboxylic Acids by Positive Mode Atmospheric Pressure Chemical Ionization Collision-Activated Dissociation Tandem Mass Spectrometry in a Linear Quadrupole Ion Trap Mass Spectrometer. *J. Am. Soc. Mass Spectrom.* **2011**, *22* (4), 670−682.

(25) Cheng, K.; Zhao, B. L.; Qi, C. Z. Silver-catalyzed decarboxylative acylation of arylglyoxylic acids with arylboronic acids. *Rsc Adv.* **2014**, *4* (89), 48698−48702.

https://doi.org/10.1021/jasms.2c00188
J. Am. Soc. Mass Spectrom. XXXX, XXX, XXX−XXX